Heterogeneous catalysis on atomic scale

Gerhard Ertl*

Fritz-Haber-Institut der Max-Planck-Gesellschaft, Faradayweg 4-6, D-14195 Berlin, Germany

Abstract

Application of scanning tunneling microscopy (STM) and other surface physical techniques to processes on well-defined single crystal surfaces enables investigations of the atomic scale steps involved in heterogeneous catalysis. Examples presented include effects caused by the operation of interactions between adsorbed particles and the role of surface defects as 'active centers'. The most detailed information is nowadays available for the CO oxidation at a Pt(1 1 1) surface. Finally, the transformation from metal to oxide will be identified as the source for the apparent 'pressure gap' in carbon monoxide oxidation on ruthenium, whereby also the concept of coordinatively unsaturated sites (cus) will be elucidated. © 2002 Elsevier Science B.V. All rights reserved.

1. Introduction

Heterogeneous catalysis is based on the interaction of the molecules involved in the reaction with the surface of the solid catalyst. In a recent essay, Boudart [1] expressed the problem as follows: "catalysis is a kinetic phenomenon. The urgent need for rate constants in heterogeneous catalysis demands the support of surface science". Instead of formulating the rate for the overall reaction on the basis of an assumed reaction mechanism, the 'surface science' approach relies on the information about the actual processes occurring on atomic scale as derived from studies with well-defined single crystal surfaces under low pressure conditions. These model systems differ, of course, appreciably from the situation encountered with 'real' catalysis, both with regards to the nature of the catalyst's surface and the applied pressure range. Attempts to overcome the "materials gap" as well as

the "pressure gap" are important tasks in this context and for most technical processes there will still be a long way ahead. Anyhow, the surface science approach is primarily able to provide detailed insights into the elementary steps underlying heterogeneous catalysis as will be demonstrated in the following by means of a few selected examples.

2. An elementary step: dissociative chemisorption

Bond breaking associated with chemisorption is one of the key processes for heterogeneous catalysis. Its principle is sketched for a diatomic molecule in Fig. 1. The well-known Lennard–Jones potential diagram illustrating the progress of this step has in reality to be replaced by six degrees of freedom which is simplified in the center of this figure by a representation in terms of two coordinates: the distance (x) of the molecule from the surface and the separation (y) between the two atoms. The height of the

* Tel.: +49-30-84135100; fax: +49-30-84135106.
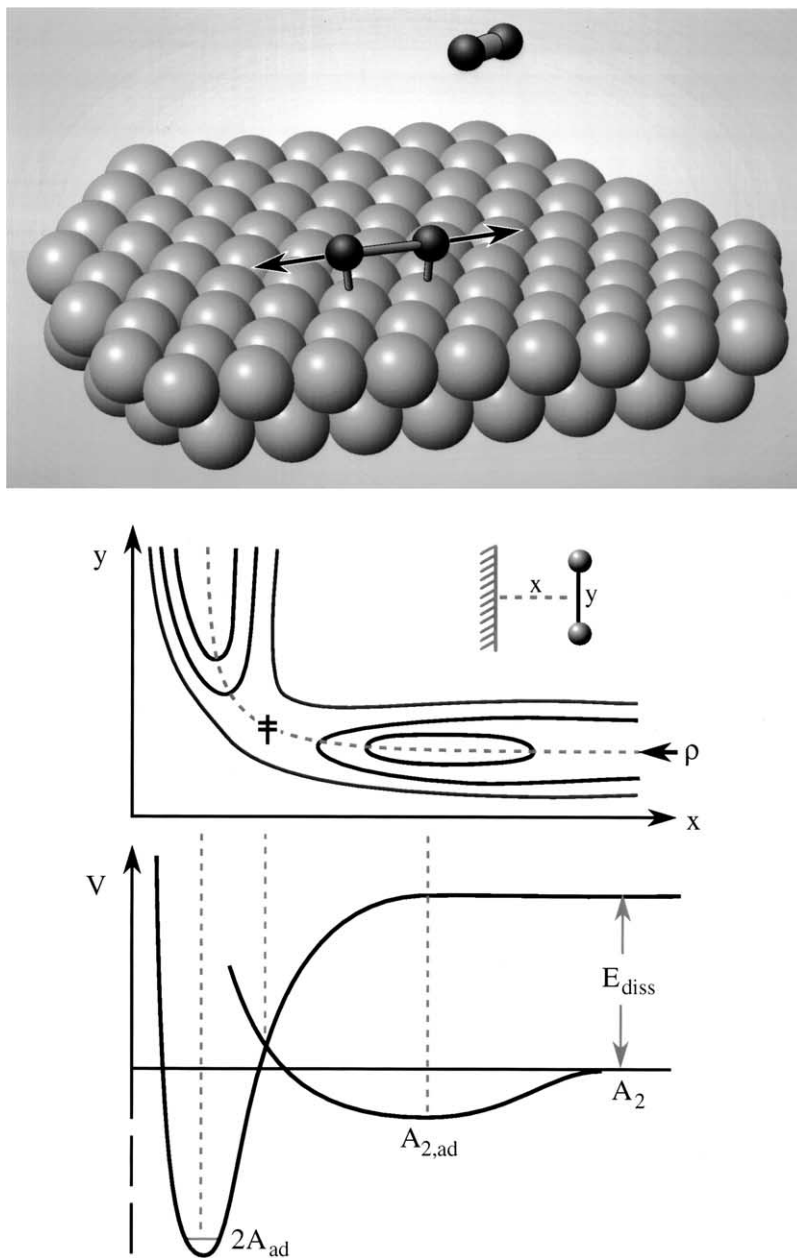*E-mail address:* ertl@fhi-berlin.mpg.de (G. Ertl).

Fig. 1. Principle of dissociative chemisorption of a diatomic molecule.

activation barrier (‡) along the reaction coordinate (ρ) determines the dissociation probability.

Fig. 2 shows a scanning tunneling microscopy (STM) image from a Pt(1 1 1) surface with atomic resolution which had been exposed to a small dose of O_2 molecules at 165 K [2]. Apart from the periodic arrangement of Pt atoms on the perfect (1 1 1) plane the image exhibits additional features, namely pairs of chemisorbed O atoms which were formed via a peroxo-like molecular "precursor" state.
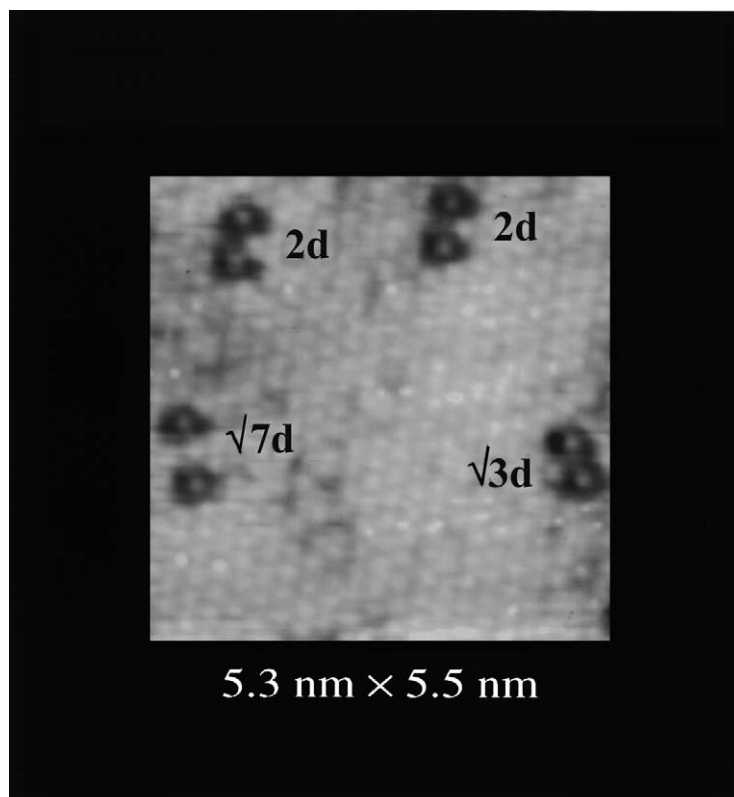
Fig. 2. STM image from a Pt(1 1 1) with chemisorbed O atoms resulting from dissociative chemisorption of O_2.

Obviously, the activation energy for this process is rather low so that it can be overcome at 165 K (but not at 100 K where adsorbed *molecules* would be discernible). The chemisorbed O atoms are located in three-fold-coordinated sites from where they can jump to neighboring sites by overcoming the activation energy for surface diffusion (E_{diff}^*). This quantity determines the residence time (τ) at a specific site for a given temperature (T), $\tau = \tau_O \exp(E_{diff}^*/k_B T)$. For the present system, the adparticles remain practically immobile at $T = 165$ K so that the image reflects their distribution after completion of the dissociative chemisorption process. Interestingly, the O adatoms are not located on adjacent sites, but are separated from each other by 0.5–0.8 nm. This is a consequence of the energy released during the dissociative chemisorption process which is preferentially channeled into motion parallel to the surface (Fig. 1). A simple estimate reveals that the time needed to

transfer this energy to the heat bath of the solid is of the order of 10^{-12} s, i.e. comparable to the period of a molecular vibration.

Fig. 2 shows further that the bright dots marking the positions of the O atoms are surrounded by dark rings. The STM technique does not simple probe the atomic locations but also the local electronic structure. In the present case, accumulation of electronic charge by the O atoms causes in turn some depletion in their intimate vicinity. This effect is responsible for the interactions between adsorbed particles mediated through the solid surface.

In order to determine the residence times of individual adparticles on specific sites at elevated temperatures, the scanning speed of the STM technique had to be increased considerably, so that now up to 20 images per second can be recorded [3]. Detailed analysis of a large set of data for O atoms chemisorbed on a Ru(0 0 0 1) surface at 300 K revealed that τ is
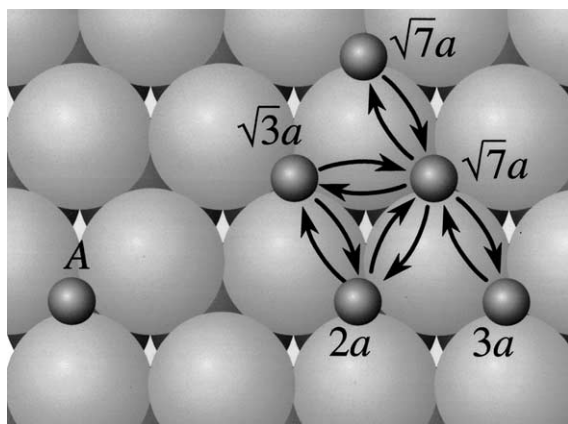
Ru(0001): Residence times at various distances d
to neighbouring adatom τ [ms] at 300 K

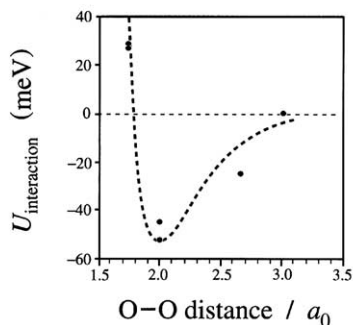| d/a_0	$\sqrt{3}$	2	$\sqrt{7}$	3	∞
τ	14	220	66	43	60

Fig. 3. Mean residence times of an O atom chemisorbed on a Ru(0 0 0 1) surface at 300 K as a function of its separation from a neighboring adatom, together with the derived interaction potential.

markedly affected by interaction with neighboring adsorbates [4]. Fig. 3 summarizes the findings about the mean residence time as a function of the distance (in units of the lattice constant, $a_0 = 0.27$ nm) to another adatom. If the latter is separated by more than $3a_0$ the interaction is negligible and $\tau = 60$ ms for an isolated particle. At an O–O distance of $2a_0$, τ becomes much longer (220 ms), while it becomes tremendously shorter at even closer separations. These effects are caused by the above mentioned operation of interactions between adsorbed particles and analysis of the present data yields an interaction potential as depicted in the lower part of Fig. 3.

The operation of interactions between adsorbed particles has several consequences. First, the residence time for an individual particle on an adsorption site will generally be affected by the momentary configuration of its neighbors and hence at finite coverages the definition of a diffusion coefficient will become rather problematic. Second, the distribution of the adsorbed particles across the surface will in general not be random (a concept underlying all formulations of reaction rates in terms of surface concentrations in the framework of a mean-field approximation), but rather give rise to the formation of ordered phases. Both aspects become evident from inspection of Fig. 4, showing a series of STM snapshots from O/Ru(0 0 0 1) with coverage $\theta = 0.1$ recorded at 300 K in intervals of 0.125 s. The surface consists now of two phases: a dense one with local coverage $\theta = 0.25$ exhibiting long-range order of a (2×2) structure (reflecting the preference of the mutual separation of $2a_0$) and a diluted one resembling a two-dimensional lattice gas with rapid and continuing fluctuations.

The examples discussed so far were concerned with processes occurring on uniform and perfect single crystal surfaces. However, any surface will contain structure imperfections and in general the activity, e.g. in bond dissociation, will be affected by the local coordination of the surface atoms involved, giving rise to the "structure sensitivity" [5]. An impressive case is offered by NO interacting with a Ru(0 0 0 1) surface [6]. Fig. 5a shows an STM image recorded 6 min after exposure of this surface to a small amount of NO at 300 K. The dark line represents a monoatomic step running across the otherwise perfect surface. (Such steps arc the most frequent structure imperfections on otherwise flat surfaces and comprise typically about 1% of the surface atoms). Near the step, dark point-like features can be seen which are identified with chemisorbed N atoms resulting from dissociation of NO. The O atoms are much more mobile (see above) and since this image was recorded on a time scale of about 1 min these show up only as faint streaks everywhere on the surface. After 120 min, the N atoms have also spread further across the surface (Fig. 5b). Obviously, dissociation takes place preferentially at the step from where the atoms formed diffuse ways. The step atoms with their lower degree of coordination act as 'active sites'—a concept introduced originally by Taylor already in 1925 [7]. This
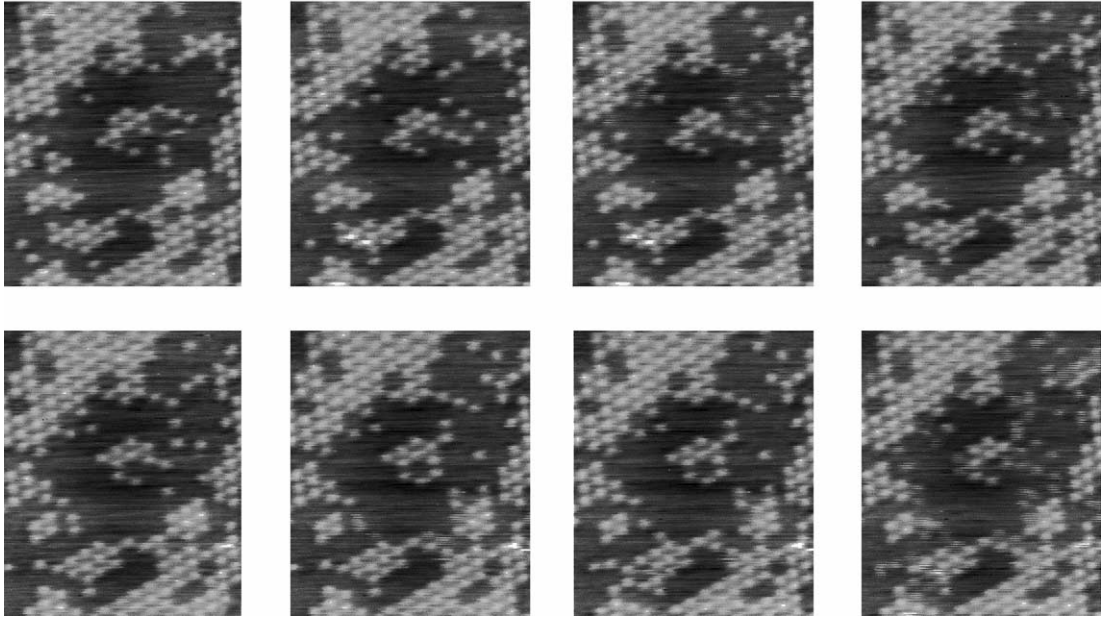
Fig. 4. A series of STM snapshots from a Ru(0 0 0 1) surface covered with chemisorbed O atoms ($\theta = 0.1$) at 300 K, taken in intervals of 0.125 s.

conclusion is also confirmed by the results of a recent theoretical study [8]. While the activation energy for dissociation of NO on a flat terrace site is 1.28 eV, it is reduced to 0.15 eV at a step site. Since, rates depend exponentially on activation energies this result demonstrates that dissociation will occur practically exclusively only at steps. Closer analysis of the experimental findings indicates that the actual situation will
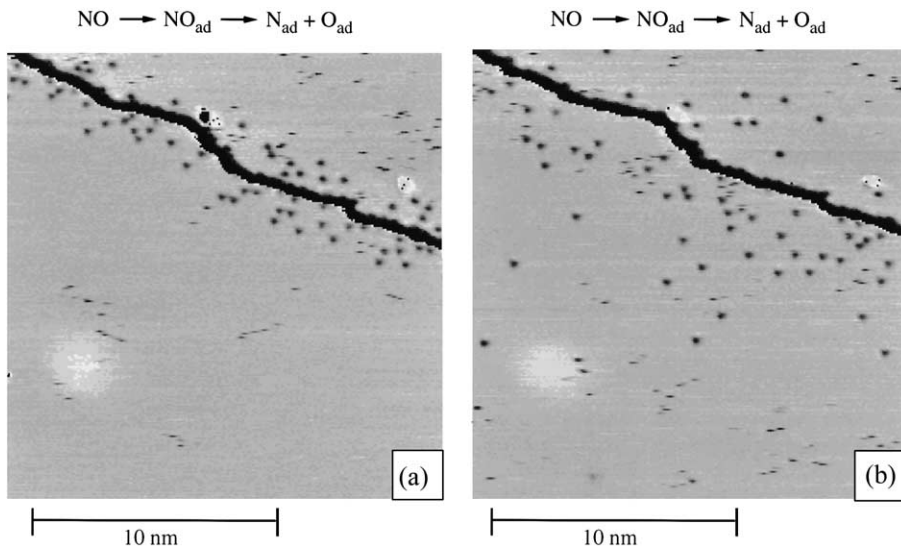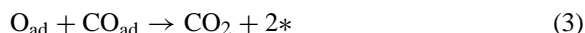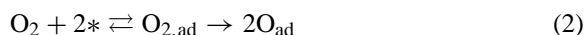
$$NO \longrightarrow NO_{ad} \longrightarrow N_{ad} + O_{ad}$$

Fig. 5. STM images from a Ru(0 0 0 1) surface with a monoatomic step after exposure to NO at 300 K: (a) 6 min; (b) 120 min after exposure.

be even more complex. It turns out that the surface in fact consists of two types of steps. One of these will be blocked by the O atoms formed and hence loose rapidly its activity, while the other type will held the O atoms less strongly so that they can diffuse away. Moreover, the number of N atoms formed per unit length of the step for a given gas exposure increases linearly with the width of the adjacent terrace. This indicates that NO molecules impinging on the terrace will there be adsorbed and diffuse rapidly until they hit a step where they will dissociate. As a consequence, the step density will not affect the overall reactivity as long as the diffusion length of NO (i.e. the mean distance this molecule travels across the surface before it desorbs again) exceeds the average separation between steps.

3. CO oxidation on Pt(1 1 1): atomic mechanism

The oxidation of carbon monoxide ($2CO + O_2 \rightarrow 2CO_2$) is catalyzed by platinum group metals and takes place via the following steps [9]:

$$CO + * \rightleftarrows CO_{ad} \tag{1}$$

$$O_2 + 2* \rightleftarrows O_{2,ad} \rightarrow 2O_{ad} \tag{2}$$

$$O_{ad} + CO_{ad} \rightarrow CO_2 + 2* \tag{3}$$

$*$ denotes schematically a free adsorption site which has, however, a quite different meaning for the two chemisorbed species involved (CO_{ad} and O_{ad}) as becomes evident from inspection of the respective adsorbate structures. These can most conveniently be

derived from analysis of low energy electron diffraction (LEED) data taken from the usually formed ordered phases as discussed above. Fig. 6a shows the structure formed on a Pt(1 1 1) surface by adsorbed CO at a coverage $\theta_{CO} = 0.75$. The CO molecules are bound to the surface via the C atom either in 'bridge' or in 'terminal' positions, quite similar as with carbonyl compounds. This arrangement represents a fairly dense packing of the adsorbate in view of its van der Waals diameter. As a consequence, a surface at this stage is no longer able to dissociatively chemisorb oxygen which process takes place according to the mechanism outlined above. It is hence necessary that under steady-state conditions the temperature is high enough (>500 K) to enable continuous thermal desorption of CO, whereby adsorption sites for oxygen become accessible.

The situation is quite different for oxygen adsorption. As with the O/Ru(0 0 0 1) system the adsorbed O atoms form the relatively open mesh of a (2×2) phase (Fig. 6b) with a coverage $\theta_O = 0.25$ with occupation of every second three-fold-coordinated site. At this stage, further uptake of oxygen is pronouncedly slowed down, but the surface is still readily able to adsorb additional CO. The resulting mixed phase is depicted in Fig. 6c and contains an 'on top' CO molecule inside the (2×2)-O unit cell.

Recombination of $O_{ad} + CO_{ad}$ leads to formation of CO_2 which is immediately released into the gas phase and hence, one might expect that this reaction takes place at random between the two species adjacent to each other in the mixed (2×2) phase. STM observation demonstrate, however, that a different progress of the reaction is preferred. Fig. 7 shows a

c(4x2) − CO   2x2 − O   2x2 − O + CO

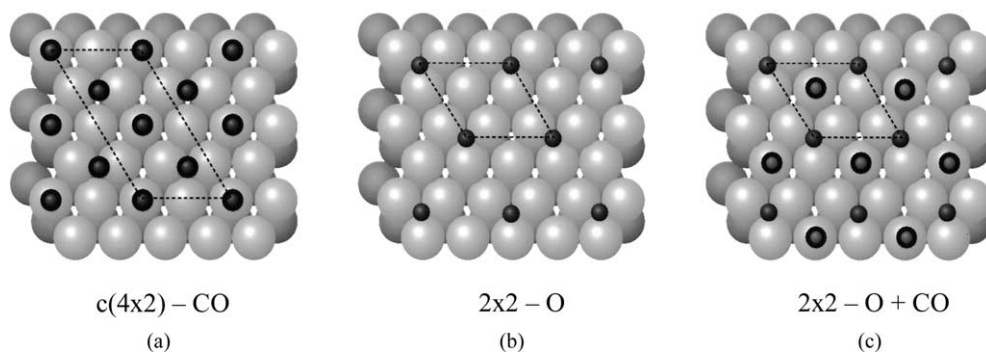(a)   (b)   (c)

Fig. 6. Ordered structures on a Pt(1 1 1) surface formed by adsorbed CO molecules and O atoms.
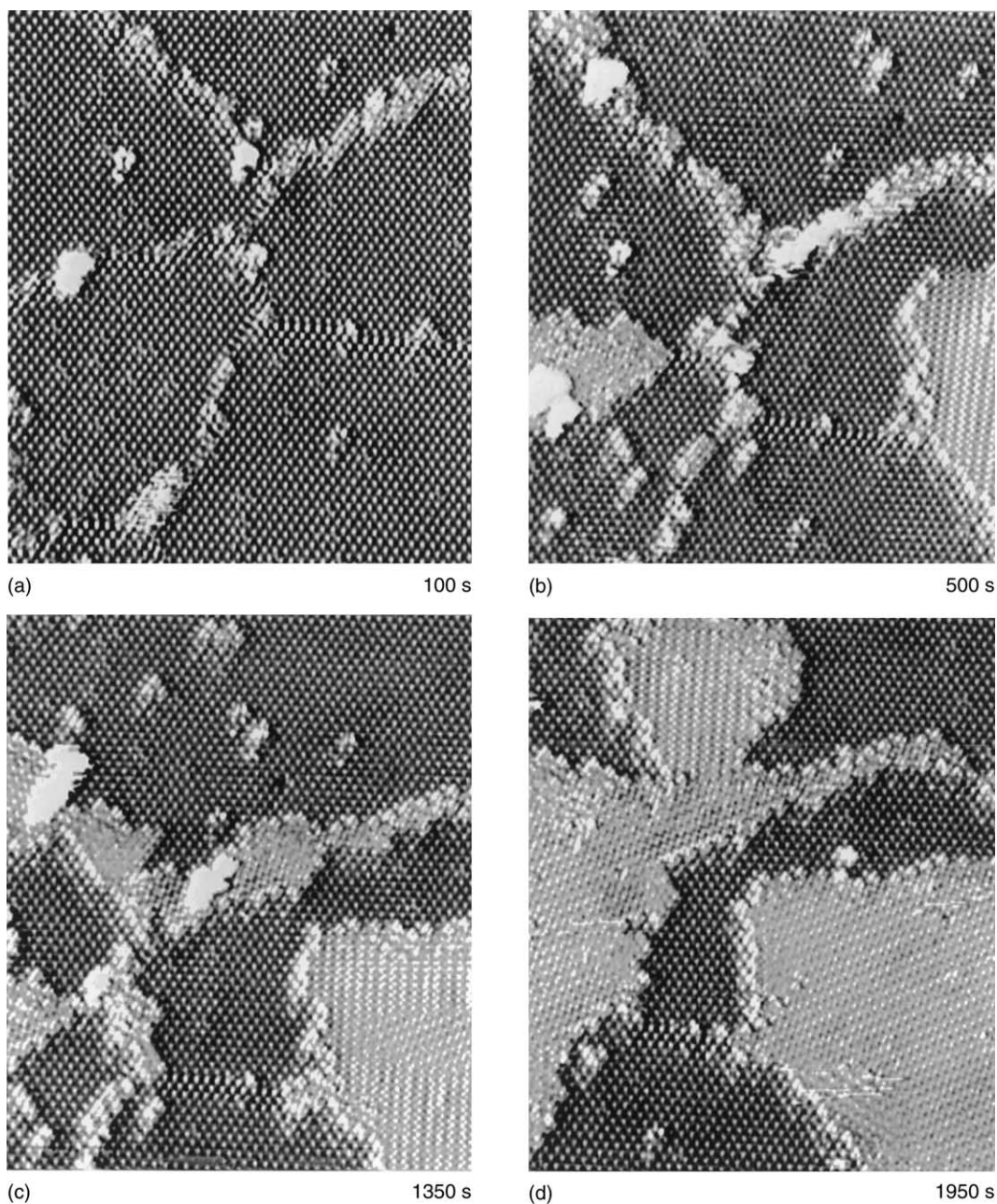
Fig. 7. A sequence of STM images from a Pt(1 1 1) surface which had been pre-covered by chemisorbed O atoms and was then exposed to CO, illustrating the progress of the catalytic reaction. $T = 244\,K$, $p_{CO} = 5 \times 10^{-7}$ mbar.

series of STM images taken at different times form a Pt(1 1 1) surface which was first completely covered by O_{ad} and then exposed to a constant CO partial pressure $p_{CO} = 5 \times 10^{-2}$ mbar at 244 K [10]. The

CO molecules at first occupy the terminal sites inside the (2×2)-O structure, but then the reaction starts at the domain boundaries of this phase (Fig. 7a). With progressing consumption of O_{ad} by the reaction
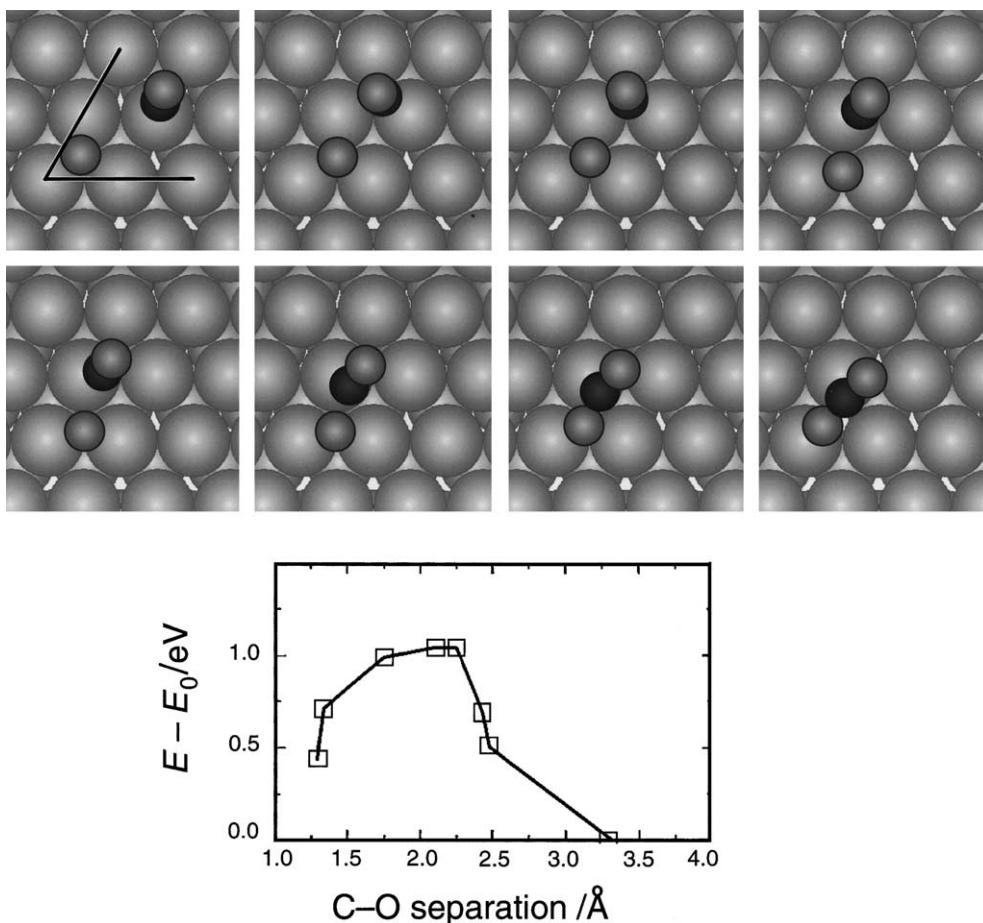
Fig. 8. Theoretical evaluation of the progress of the reaction $O_{ad} + CO_{ad}$ [11].

the empty sites are occupied by the impinging CO molecules which form continuously growing patches of the CO-c(4×2) phase (Fig. 7b–d) whose structure is depicted in Fig. 6a. Obviously the reaction does preferentially take place at the boundaries of O-covered islands and not randomly inside the mixed phase.

The explanation for this behavior is provided by the results of recent density functional theory (DFT) calculations [11]. Fig. 8 shows the variation of the energy as a function of the distance between O_{ad} (initially in a three-fold-coordinated site) and CO_{ad} (initially in a nearby 'on top' site) reflecting the progress of the reaction. The activation energy for starting with this configuration turns out to be 1.0 eV, in perfect agreement with the value determined experimentally for a situation with low coverages, i.e. initially well

separated adsorbates, while at higher coverages this number was found to be considerably smaller, namely only 0.5 eV [12]. This latter value results from theory if the reaction starts instead with the second type of configuration where the CO molecule is in a bridge-type position near the O atoms. This kind of arrangement is just found at the domain boundary of a c(4×2)-CO phase progressing towards the mixed O + CO-(2×2) phase and therefore, the reaction occurs preferentially through such a mechanism. Under steady-state flow conditions, the reaction will proceed at fluctuating phase boundaries with constant fractions (determined by the partial pressures and temperature) being covered by each of the two phases. At higher temperatures, disorder increases leading eventually to quasi-random distribution.

The sketched phenomenon (being caused by the operation of interactions between adsorbed particles) affects also the kinetics. Description of the rate in terms of the mean-field expression $R = k\theta_O\theta_{CO}$ fails and should be replaced by $R = k'L$, where L is the total length of the domain boundaries. Detailed analysis of the STM data revealed, however, that the former represents still a good approximation over an intermediate coverage range [10]. It is felt that such a situation will frequently be found even with the complex situation of 'real' catalysis, whereby the Langmuir-type rate equations underlying microkinetics become microscopically justified.

4. The 'pressure gap': CO oxidation on ruthenium

The findings at the low pressures on the mechanism of CO oxidation with Pt or Pd single crystal surfaces can be safely transferred to the conditions of 'real' catalysis with supported catalysts at atmospheric pressure [13]. With Ru, however, the situation is rather
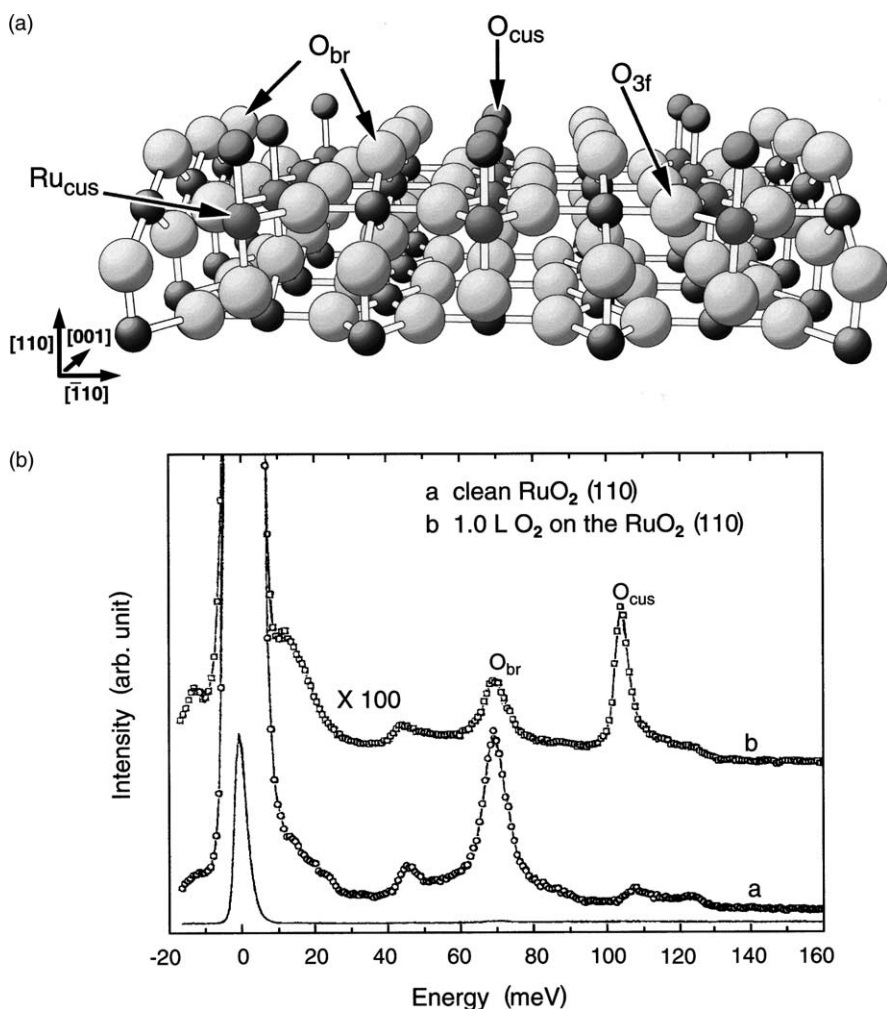

Fig. 9. (a) Structure model of the $RuO_2(1\,1\,0)$ surface with O atoms both in bridge positions (O_{br}) and on coordinatively unsaturated sites (O_{cus}); (b) vibrational spectra recorded by high resolution electron energy loss spectroscopy (HREELS).

puzzling. In low pressure studies with Ru single crystal surfaces this metal is practically completely inactive [9], but at atmospheric pressure with supported catalysts the activity of this element exceeds that of Pt or Pd by far [14]. This effect is not governed by differences of the surface structure if a Ru(0 0 0 1) single crystal surface is compared with a supported Ru/SiO$_2$ catalyst [15] and is thus, a clear example for the so-called "pressure gap". The inactivity of (metallic) Ru has to be attributed to the stronger (compared with Pt) chemisorption energy of O, which as a consequence increases the activation energy for step (3), O$_{ad}$+CO$_{ad}$ → CO$_2$, so that instead thermal desorption of CO is favored. The binding energy of O decreases continuously with increasing coverage up to completion of a full monolayer with $\theta_O = 1$ [16], but at the same time CO adsorption becomes inhibited, so that for $\theta_O > 0.5$ no CO is held on the surface any more at temperatures above 100 K [17]. Hence, CO$_2$ formation will be suppressed because of the lack of adsorbed CO. Exposure of a Ru(0 0 0 1) surface to large doses of O$_2$ (e.g. 1 mbar for several seconds) at elevated temperatures, however, causes further oxygen uptake and the resulting phase adsorbs CO at room temperature and readily catalyzes its oxidation (even at low pressures) [18]. This is obviously the situation encountered in an atmosphere of elevated oxygen pressure. Detailed investigations using STM, LEED and DFT calculations revealed that this 'oxygen rich' phase is in fact RuO$_2$ which grows epitaxially with its (1 1 0) plane parallel to the Ru(0 0 0 1) surface [19]. Fig. 9a shows the derived structure model of this surface with additional

(weakly held) O atoms adsorbed on coordinatively unsaturated Ru atoms. This species shows up in the vibrational spectrum (Fig. 9b) as an additional peak at 103 meV while the bridge bonded O$_{br}$ species forms part of the substrate lattice and exhibits a vibrational band at 69 meV [20]. The concept of coordinatively unsaturated sites (cus) was introduced long ago by Burwell et al. to account for the catalytic activity of oxides [21] and is here directly experimentally confirmed. These sites are usually not saturated by O$_{ad}$ and can also accommodate adsorbed CO (Fig. 10). CO is oxidized already at 300 K through reaction with both the O-cus as the O-bridge species. The O-vacancies created in the latter case may in turn be occupied by CO, whereby CO is more strongly held in bridge than in cus positions. Catalytic reaction under steady-state flow conditions takes place at temperatures as low as 300 K [22]. As an example, Fig. 11 shows the variation of this rate with p_{CO}, at fixed $T = 350$ K and $p_{O_2} = 10^{-7}$ mbar [23]. At first r increases with p_{CO} up to a maximum which is reached near the point where $p_{CO} = 2p_{O_2}$, i.e. for the stoichiometric composition. The decrease with further increase of p_{CO} is attributed to progressing blocking of the cus sites by CO$_{ad}$, whereby oxygen adsorption becomes inhibited.

Comparably high activities in catalytic CO oxidation down to room temperature were recently reported for experiments performed at atmospheric pressure with small RuO$_2$ particles prepared from aqueous solution [24], so that there is now strong evidence that with this system the pressure gap could be bridged and a long standing puzzle could be solved.
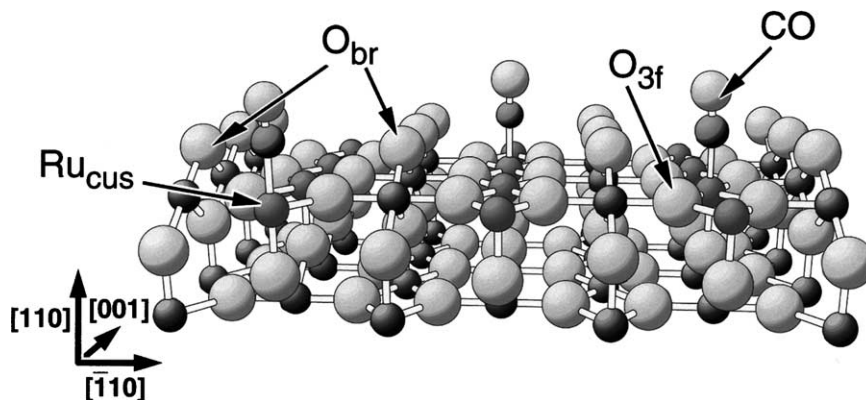

Fig. 10. Structure model of the RuO$_2$(1 1 0) surface with CO molecules adsorbed on cus-sites.
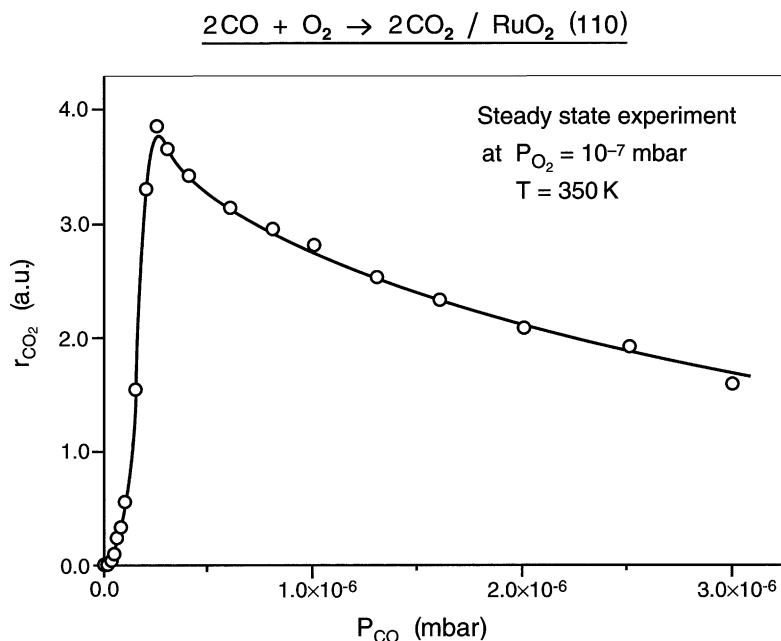
$2\,CO + O_2 \rightarrow 2\,CO_2$ / RuO_2 (110)

Steady state experiment
at $P_{O_2} = 10^{-7}$ mbar
$T = 350\,K$

r_{CO_2} (a.u.)

P_{CO} (mbar)

Fig. 11. Rate of CO_2 production under steady-state flow conditions on a $RuO_2(1\,1\,0)$ surface as a function of CO partial pressure at fixed $T = 350\,K$, $p_{O_2} = 10^{-7}$ mbar.

5. Conclusions

The macroscopic kinetics of a heterogeneously catalyzed technical process will be governed by the microscopic elementary processes occurring on atomic scale and which are now accessible to detailed investigation by applying the arsenal of modern surface physics to well-defined single crystal surfaces operated under low pressure conditions. The examples presented were intended to demonstrate the degree of sophistication which can now be reached. Even with the apparently simple systems treated here the high degree of complexity becomes evident. Only a few further aspects not treated here will be briefly listed:

(i) Under working conditions the composition and structure of the surface of a catalyst will frequently undergo profound alterations, i.e. the reaction 'digs its own bed'.

(ii) Even very small amounts of additional elements may have marked effects on the reactivity, either as promoters or as poisons.

(iii) Under steady-state flow conditions the reaction rate may become oscillatory or even chaotic.

These effects are a consequence of the non-linear character of the underlying kinetic equations and are usually associated with the development of spatio-temporal concentration patterns on mesoscopic scale.

(iv) Any chemical transformation is the result of transfer of energy between the different degrees of freedom in the reacting system. These effect became recently accessible to experimental investigation through application of ultrashort laser techniques.

It is felt that the 'surface science' approach, as originally suggested by Langmuir [25], will be of fundamental significance also in future attempts to solve the sketched problems, whereby further light will be shed on the complex phenomenon of heterogeneous catalysis.

References

[1] M. Boudart, Catal. Lett. 65 (2000) 1.
[2] J. Wintterlin, R. Schuster, G. Ertl, Phys. Rev. Lett. 77 (1996) 123.

[3] J. Wintterlin, J. Trost, S. Renisch, R. Schuster, T. Zambelli, G. Ertl, Surf. Sci. 394 (1997) 159.

[4] S. Renisch, R. Schuster, J. Wintterlin, G. Ertl, Phys. Rev. Lett. 82 (1999) 3839.

[5] M. Boudart, Adv. Catal. 20 (1969) 153.

[6] T. Zambelli, J. Wintterlin, J. Trost, G. Ertl, Science 273 (1996) 1688.

[7] H.S. Taylor, Proc. R. Soc. London A 108 (1925) 105.

[8] B. Hammer, Phys. Rev. Lett. 83 (1999) 368.

[9] T. Engel, G. Ertl, Adv. Catal. 28 (1979) 1.

[10] J. Wintterlin, S. Völkening, T.V.W. Janssens, T. Zambelli, G. Ertl, Science 278 (1997) 1931.

[11] A. Alavi, P. Hu, T. Deutsch, P.L. Silvestrelli, J. Hutter, Phys. Rev. Lett. 80 (1998) 3650.

[12] C.T. Campbell, G. Ertl, H. Kuipers, J. Segner, J. Chem. Phys. 73 (1980) 5862.

[13] (a) S.H. Oh, G.B. Fisher, J.E. Carpenter, D.W. Goodman, J. Catal. 100 (1986) 360;
(b) S. Ladas, H. Poppa, M. Boudart, Surf. Sci. 102 (1981) 151.

[14] N.W. Cant, P.C. Hicks, B.S. Lennon, J. Catal. 24 (1984) 372.

[15] C.H. Peden, D.W. Goodman, J. Phys. Chem. 90 (1980) 1360.

[16] C. Stampfl, S. Schwegmann, H. Over, M. Scheffler, G. Ertl, Phys. Rev. Lett. 77 (1996) 3371.

[17] F.M. Hoffmann, M.D. Weisel, C.H.F. Peden, Surf. Sci. 253 (1991) 59.

[18] A. Böttcher, H. Niehus, S. Schwegmann, H. Over, G. Ertl, J. Phys. Chem. B101 (1997) 111185;
A. Böttcher, H. Niehus, S. Schwegmann, H. Over, G. Ertl, J. Phys. Chem. B103 (1999) 6267.

[19] H. Over, Y.D. Kim, A.P. Seitsonen, S. Wendt, E. Lundgren, H. Schmid, P. Varga, A. Morgante, G. Ertl, Science 287 (2000) 1474.

[20] Y.D. Kim, A.P. Seitsonen, S. Wendt, J. Wang, C. Fan, K. Jacobi, H. Over, G. Ertl, J. Phys. Chem. 105 (2001) 3752.

[21] R.L. Burwell, G.L. Haller, K.C. Taylor, J.F. Read, Adv. Catal. 20 (1969) 1.

[22] C.Y. Fan, J. Wang, K. Jacobi, G. Ertl, J. Chem. Phys. 114 (2001) 10058.

[23] C.Y. Fan, J. Wang, K. Jacobi, G. Ertl, in preparation.

[24] L. Zang, H. Kisch, Angew Chem. 112 (2000) 4075.

[25] I. Langmuir, Trans. Farad. Soc. 17 (1922) 607.